Original Research Article

Senolytics rejuvenate the reparative activity of human cardiomyocytes and endothelial cells

Piotr Sunderland[1], Lulwah Alshammari[1], Emily Ambrose[1], Daniele Torella[2], Georgina M. Ellison-Hughes[1] iD

[1]Centre for Human and Applied Physiological Sciences, School of Basic and Medical Biosciences, Faculty of Life Sciences & Medicine, King's College London, Guy's Campus, London SE1 1UL, UK.
[2]Molecular and Cellular Cardiology, Department of Experimental and Clinical Medicine, Magna Graecia University, Catanzaro 88100, Italy.

Correspondence to: Dr. Georgina M. Ellison-Hughes, Centre for Human and Applied Physiological Sciences, School of Basic and Medical Biosciences, Faculty of Life Sciences & Medicine, Guy's Campus, King's College London, London SE1 1UL, UK. E-mail: georgina.ellison@kcl.ac.uk

Abstract

Introduction: Senescent cells have emerged as bona fide drivers of ageing and age-related cardiovascular disease, with senescent cells accumulating in the aged heart and following damage/injury. We have shown that the removal of senescent cells using senolytics can rejuvenate the regenerative capacity of the aged heart.

Aim: To investigate the effects of cell senescence and the action of the senolytics, Dasatinib (D) and Quercetin (Q) on human iPSC-derived cardiomyocyte survival and cell cycle, and endothelial cell survival, cell cycle, migration and tube formation *in vitro*.

Methods and Results: We developed a transwell insert co-culture stress-induced premature senescence human cell model system to test the effects of senolytics D+Q *in vitro*. Co-culture of iPSC-derived cardiomyocytes (iPSC-CMs) with senescent cardiac stromal progenitor cells (senCPCs) led to decreased number and DNA-synthesising activity of iPSC-CMs. Treatment with senolytics D+Q led to the elimination of senCPCs in the co-culture and the rescue of iPSC-CM number and DNA synthesis. Treatment of HUVECs with senCPC conditioned media decreased HUVEC number, cell cycle activity, migration, and tube formation. Treatment of HUVECs with D+Q conditioned media rescued HUVEC number, migration and tube formation. Next, we investigated the effects of co-culture of senescent HUVECs (senHUVECs) with HUVECs and showed decreased HUVEC number and DNA synthesis.

Treatment with senolytics D+Q led to the elimination of senHUVECs in the co-culture and ameliorated HUVEC number, but not DNA synthesis. Treatment of HUVECs with conditioned media from senHUVECs led to decreased HUVEC migration and tube formation. Treatment of HUVECs with D+Q conditioned media improved HUVEC tube formation but not migration. Luminex analysis of the conditioned media from iPSC-CM and HUVEC co-cultures revealed upregulation of senescence-associated secretory phenotype (SASP) factors, but the level of SASP factors was reduced with the application of D+Q.

Conclusion: Senescent cell removal by senolytics D+Q shows therapeutic potential in rejuvenating the reparative activity of human cardiomyocytes and endothelial cells. These results open the path to further studies on using senolytic therapy in age-related cardiac deterioration and rejuvenation.

Potential impact of the findings: Senescent cells and their SASP present a promising therapeutic target to rejuvenate the heart's reparative potential. Clinical trials using senolytics D+Q are already underway and thus far have shown promising results. Further pre-clinical studies are warranted for evidence-based clinical trials using senolytics in age-related cardiovascular diseases.

Keywords: Cell senescence, senolytics, iPSC-derived cardiomyocytes, endothelial cells, cardiovascular

INTRODUCTION

The world's population is ageing rapidly, and people are living longer. By 2050, the number of people aged 65 years or over worldwide is expected to more than double, reaching over 1.5 billion persons, meaning that one in six people globally will be ≥ 65 years[1]. Despite unparalleled advances in prevention, diagnostics, and treatment, increased life expectancy will result in a higher incidence of multiple chronic conditions and disabilities (multi-morbidity). Ageing is the greatest risk factor for many life-threatening disorders, including cancer, cardiovascular disease, and neurodegeneration. Basic ageing processes or hallmarks drive the functional and cellular deterioration of most organs and tissues, predisposing them to the onset and progression of disease and pathology. Interventions that target these basic mechanisms and regenerate tissues and organs are urgently needed to prevent and reverse age-related damage and disease[2].

One hallmark of ageing is cell senescence, which is a detrimental cell state triggered by stressful insults and certain physiological processes (i.e., oxidative stress), whereby damaged cells exit the cell cycle permanently and remain metabolically active. A key feature of senescent cells is that they produce and secrete pro-inflammatory factors, termed the senescence-associated secretory phenotype (SASP). Long-term persistence of senescent cells and their SASP disrupts tissue structure and function with deleterious paracrine/autocrine and systemic effects[3,4]. Accumulation of senescent cells in tissues, including the heart, with ageing and at etiological sites in multiple chronic diseases is detrimental, contributing to pathophysiology and organ deterioration[3-8]. Altogether the accumulation of senescent cells with ageing and disease, including cardiovascular disease, have been causally linked to decreased lifespan and healthspan[3-8].

We and others have shown that eliminating senescent cells using senolytics (Navitoclax, Dasatanib+Quercetin) or genetic (using INK-ATTAC+AP mice) clearance of senescent cells in aged mice alleviated detrimental features of cardiac ageing, including myocardial dysfunction, hypertrophy and fibrosis, and induced a compensatory cardiomyocyte renewal and replacement[9-11]. Our group was the first to show that eliminating senescent cells in aged mice using the senolytics Dasatanib+Quercetin (D+Q) rejuvenated the heart's regenerative potential, with progenitor cell activation, new cardiomyocyte formation, and improved cardiac function[9].

To test the effects of senescence and senolytics *in vitro*, we have developed a transwell-based stress-induced premature senescence co-culture human cardiac cell model system[9]. In the present study, we investigate the effects of cell senescence and the action of the senolytics D+Q on human cardiomyocyte and endothelial cells *in vitro*.

MATERIALS AND METHODS

Human CPC isolation

c-kit positive cardiac progenitor cells (CPCs) were isolated as previously described[9,12]. A right atrial appendage myocardial sample (~200 mg) was obtained from a male subject with cardiovascular disease undergoing valve replacement surgery. The subject gave informed consent to take part in the study (NREC #08/H1306/91). Briefly, cardiac tissue was minced and then digested with collagenase II (0.3 mg/mL; Worthington Laboratories) in Dulbecco's Modified Eagle's Medium (DMEM; Sigma-Aldrich) at 37 °C in a series of sequential digestions for 3 min each. Enzymatically released cells were filtered through a 40 μm cell strainer (Becton Dickinson, BD) and collected in enzyme quenching media (DMEM + 10% FBS). The isolated cardiac cells were collected by centrifugation at 400 g for 10 min, resuspended in incubation media (PBS, 0.5% BSA, 2 mM EDTA), and passed through an OptiPrep™ (Sigma-Aldrich) density gradient medium to remove large debris. This involved layering the cardiac cell population on top of 16% and 36% OptiPrep™:DMEM solutions and then centrifuging for 20 min at 800 g with no brake. Larger debris is collected at the bottom of the tube, allowing for selective retrieval of the small cell fraction from the upper layers. For the isolation of c-kit^{pos}, CD45^{neg}, and CD31^{neg} CPCs, first, the small cardiac cells were depleted of CD45^{pos} and CD31^{pos} cells by immunolabelling with anti-human CD45 and CD31 magnetic immunobeads (Miltenyi) diluted (1:10) in incubation media for 30 min at 4 C with agitation. After antibody binding, the CD45^{pos}/CD31^{pos} cells were depleted from the preparation using magnetic activated cell sorting (MACS; Miltenyi). The elution cells, which were CD45^{neg}, CD31^{neg} were then enriched for c-kit^{pos} cardiac cells through incubation with anti-human CD117 immunobeads (Miltenyi) (1:10) for 30 min at 4 C with agitation and again sorted using MACS according to the manufacturer's instructions.

Cell culture

Early passage human CPCs were cultured on CellStart-coated (Life Technologies) cultureware in a growth medium containing 45% DMEM/F12 Ham (Sigma-Aldrich), 1 X ITS (Life Technologies), 45% Neurobasal Medium (Life Technologies), 0.5% Glutamax (Life Technologies), 1 X B27 (Life Technologies),1 X N2 (Life Technologies), 20 ng/mL epidermal growth factor (EGF) (Peprotech), 10 ng/mL basic fibroblast growth factor (bFGF) (Peprotech), 10% Stemulate human platelet lysate (Cook Medical), 10 ng/mL leukemia inhibitory factor (LIF) (Millipore), 1% PenStrep (Life Technologies), 0.1% Fungizone (Life Technologies), and 0.1% Gentamicin (Sigma-Aldrich). CPCs were grown at 37 °C in 5% CO_2 and 2% O_2.

Early passage HUVECs (Lonza) were cultured in EBM-Plus medium (Lonza) supplemented with 2% FBS (Lonza), 0.1% Hydrocortisone (Lonza), 0.1% Ascorbic acid (Lonza), 0.1% rhEGF (Lonza), 0.1% Gentamicin (Lonza), 0.1% Heparin (Lonza), 0.5% Fungizone (Lonza), 5% L-Glutamine (Lonza), and 0.2% BBE (Lonza). HUVECs were grown at 37 °C in 5% CO_2 and 19% O_2.

Human iPSC-derived Ventricular Cardiomyocytes (iPSC-CMs) (Axol) were plated on Fibronectin-coated plates (Thermo Fisher Scientific) in Plating Medium containing 90% Axol Maintenance Medium (Axol Cardiomyocyte Basal Medium with Axol Cardiomyocyte Supplement), 10% FBS (Lonza) and 10 μM ROCK inhibitor (Y-27632). After 24 h, cells were maintained in Maintenance Medium only. Cardiomyocytes were used for experiments after 5 days when beating occurred. Cardiomyocytes were verified by

immunofluorescence staining for Anti-α-Actinin (Sarcomeric) using antibody, Mouse monoclonal (Sigma, A7732).

Induction of cells to senescence

Doxorubicin was added to the growth medium in a final concentration of 0.2 μm for 24 h to induce cells to senescence[9]. After that time, cells were washed with PBS and maintained in culture for a further 21 (HUVECs) or 28 days (CPCs) for cells to reach a deep senescent state[9]. Quantification of senescence was carried out on three independent replicates/wells by counting the number of SA-β-gal stained cells in 10 fields of view per well and expressed as a percentage of the total number of cells.

Transwell insert co-culture model system *in vitro*

Doxorubicin induced senescent CPCs (senCPCs) or HUVECs (senHUVECs) were seeded in the bottom chamber. Human iPSC-cardiomyocytes (iPSC-CMs) or HUVECs were seeded on the top chamber insert. Co-cultures were left for 7 days and then iPSC-CMs or HUVECs in the top chamber were analysed for cell number by crystal violet staining, BrdU cell cycle and markers of senescence, and the conditioned medium analysed for SASP factors[9]. The cultures were then treated with senolytics, dasatinib (D; 0.5 μM) and quercetin (Q, 20 μM Q) (D+Q) for 3 days to clear the senescent cells in the bottom chamber[9]. Then 7 days later, the iPSC-CMs or HUVECs in the top chamber were analysed for cell number by crystal violet staining, BrdU cell cycle, the markers of senescence, and conditioned medium analysed for SASP factors (total of 17 days). Control was iPSC-CMs or HUVECs cultured alone on the top chamber insert, with no cells on the bottom chamber. Three independent replicates/wells were used per assay and condition.

Crystal Violet staining

Membrane inserts or wells containing adherent cells were washed twice with PBS and fixed with ice-cold methanol for 10 min. Cells were then covered with 0.5% solution of crystal violet (Sigma-Aldrich) in 25% methanol for 10 min at room temperature. Cells were washed once with distilled water and left to dry at room temperature. For quantification, 10 random fields of view were photographed for each insert or well ($n = 3$) with a light microscope (OLYMPUS CKX41). The percentage area occupied by purple crystal violet stained viable, adherent cells was measured in ImageJ software[9]. Results were presented as a percentage of control (normal growth medium) inserts or wells.

BrdU proliferation assay

To label cells in the S phase of the cell cycle, BrdU (Roche) was added to the culture media in a final concentration of 10 μM. After 12 h (HUVECs) or 24 h (iPSC-CM), cells were fixed in ice-cold solution of 15 mM glycine in 70% ethanol and stored at -20 °C. Cells were then stained using a BrdU detection kit (Roche) by washing three times with the provided washing buffer and incubating with primary anti-BrdU antibody diluted 1:10 in incubation buffer for 30 min at 37 °C. Following three washes in washing buffer, secondary anti-mouse fluorescein antibody in 1:10 dilution was added for 30 min at 37 °C. Nuclei were stained with DAPI solution (Thermo Fisher Scientific) for 10 min, and after two final washes, cells were mounted to glass coverslips. For quantification, 10 images of random fields of view for each insert ($n = 3$) were taken with a fluorescence microscope (Nikon). The number of BrdU-positive cells was counted and expressed as a percentage of total DAPI nuclei.

SA-β-gal staining

Cells were stained using Senescence β-Galactosidase Staining Kit (Cell Signalling). Media was removed and cells were washed with PBS and fixed with Fixative Solution for 10 min. Cells were then washed twice with PBS and covered with staining solution containing 1 mg/mL X-Gal in pH = 6. The well plate or insert was sealed and placed at 37 °C overnight. After the staining solution had been removed, nuclei were counterstained using DAPI (Thermo Fisher Scientific) for 10 min. For quantification, images were acquired

of 10 random fields of view per well or insert (n = 3) using a brightfield and fluorescence microscope (Nikon). Cells that stained deep blue were counted as positive, and results were expressed as a percentage of total DAPI nuclei or cells.

Immunocytochemistry

Cells were fixed with 4% paraformaldehyde for 10 min, then washed with PBS twice. 0.4% Triton X-100 (Sigma-Aldrich) was used for 10 min to permeabilize the cell membrane. For blocking, 2% BSA, 1.5% donkey serum and 0.1% Triton solution in PBS was used for 10 min. The primary antibody for p21 (Santa Cruz Biotechnologies sc-6246, mouse monoclonal) or Ki67 (Abcam ab15580, rabbit polyclonal) was diluted (1:500) in blocking buffer and cells were incubated for 2 h at room temperature. Then cells were washed for 5 min with PBS three times. Alexa Fluor 543 secondary antibody (Thermo Fisher Scientific) diluted in PBS at a 1:1,000 dilution was incubated with the cells for one hour at room temperature. Then cells were washed for 5 min with PBS three times. Nuclei were counterstained using DAPI at 1:1,000 dilution (Thermo Fisher Scientific) in PBS for 10 min, then washed once with PBS, then distilled water for 5 min each. Cells on inserts (p21) or coverslips (Ki67) were mounted on slides using VectaMount mounting medium. For quantification, 10 images of random fields of view for each insert or coverslip (n = 3) were taken with a fluorescence microscope (Nikon). The number of p21-positive or Ki67-positive cells was counted and expressed as a percentage of total DAPI nuclei.

Tube formation assay

96-well plates were covered with 100 μL/cm² Geltrex (Gibco) for 30 min at 37 °C. HUVECs were suspended in a normal HUVEC growth medium, counted and divided into aliquots of 40,000 cells. Each aliquot was then centrifuged at 200 × g and resuspended in 200 μL of chosen conditioned medium (senHUVEC or senCPC conditioned medium, D+Q-conditioned medium (HUVEC or CPC), normal growth medium) to a density of 200,000 cells/mL. 65 μL/well of each suspension was then placed in the Geltrex-covered 96-well plate and left in the incubator overnight at 37 °C in 5% CO_2 and 19% O_2. Cells were fixed in ice-cold ethanol for 10 min and photographed in phase contrast (OLYMPUS CKX41). The sum of the length of tubes formed in each well (n = 3) was calculated and results were presented as a percentage of control wells (normal growth medium).

Cell migration scratch assay

200,000 HUVECs were plated into a 6-well plate with normal growth media (EBM-plus supplements). Once 90%-100% confluent, the media was changed to serum-starvation media (EBM with no supplements or FBS) and incubated overnight at 37 °C in 5% CO_2 and 19% O_2. The next day, the serum starvation media was aspirated and a scratch was performed on the cell monolayer down the centre of each well using a p200 pipette tip. Any debris was removed by washing twice with warm EBM-plus. To enable imaging the area with scratch injury, the location of the scratch of at least three reference points per well was marked using an ultrafine tip marker on the outer bottom of the culture plate. Pictures were taken of the reference points at 4× magnification (OLYMPUS CKX41). Then scratched cells in wells were supplemented with the chosen conditioned media [senHUVEC or senCPC conditioned medium, D+Q-conditioned medium (HUVEC or CPC), normal growth medium (EBM-plus)] and left in the incubator at 37 °C in 5% CO_2 and 19% O_2 for 24 h. After 24 h, cells were washed twice with PBS to gently remove detached or dead cells. Then scratched areas within each well were re-imaged at each reference point. Images were uploaded to Fiji Image J software and the number of migrated cells that crossed into the scratched area from their reference point was quantified. Three independent replicates/wells were carried out per condition. Results were presented as a percentage of control wells (normal growth medium).

Multiplex luminex immunoassay

Conditioned culture media was collected from the different co-culture conditions (CTRL 7 days, Co-Culture 7 days, CTRL 17 days, Co-culture 17 days and Co-culture D+Q 17 days) for both senCPC/iPSC-CM and senHUVEC/HUVEC co-culture experiments. 2 × independent replicate aliquots of each conditioned media condition was centrifuged at 1,000 × g at 4 °C. Multiplex Luminex immunoassay kits for 8 SASP factors (IL-6, IL-8, CCL11, CXCL5, CXCL1, CCL7, IL-1β and TNFα) were purchased from R&D systems. Capture beads were magnetically immobilised on a microplate and washed with the provided washing buffer. Conditioned media samples were added to the beads and incubated for 2 h at room temperature with shaking. Following two washes with washing buffer, a biotinylated detection antibody mix was added to the plate and incubated for 2 h at room temperature with shaking. The plate was then washed twice and Streptavidin-PE was added to the beads-antibodies complex for 30 min of incubation. After the final wash step, beads were suspended in the provided reading buffer and analysed using Luminex FlexMAP 3D instrument with a DD gate set at 7,500-25,000 and a minimum bead count of 50. Results were compared to antigen standards prepared on the same plate in 7 serial dilutions and the level of protein secretion was measured.

Statistical analysis

Data are Mean ± SD. The data displayed normal variance. Significance between the two groups was determined by Student's t-test and in multiple comparisons by the analysis of variance (ANOVA) using GraphPad Prism (GraphPad Software). In the event that ANOVA justified post-hoc comparisons between group means, these were conducted using Tukey's multiple-comparisons test. $P < 0.05$ was considered significant.

RESULTS

Co-culture with senCPCs decreases the number of iPSC-CMs and their cell cycle activity

The phenotype of iPSC-CMs was verified by staining positive for sarcomeric α-actinin and beating [Supplementary Figure 1]. We have previously shown that 0.2 μm doxorubicin (dox) for 24 h induces human stromal cardiac progenitor cells (CPCs) into a deep senescent state (~80%) after 35 days post-dox treatment[9]. Similarly, we show here that 0.2 μm dox for 24 h induces ~80% of human CPCs to express SA-β-gal activity after 28 days post-dox treatment [Supplementary Figure 2]. Co-culture of iPSC-CMs with senescent CPCs (senCPCs) for 7 days led to decreased ($P < 0.01$) number of iPSC-CMs shown through crystal violet viability staining, compared to iPSC-CMs cultured alone (CTRL) [Figure 1A]. Co-culture with senCPCs also decreased ($P < 0.05$) iPSC-CM DNA synthesis, compared to iPSC-CMs cultured alone (CTRL) [Figure 1B]. There was no change in senescence markers, SA-β-Gal activity or p21 expression, in iPSC-CMs co-cultured with senCPCs [Figure 1C and D].

Senolytics D+Q rescue iPSC-CM number and cell cycle activity

We have previously shown that the senolytics D (at a concentration of 0.5 μM) + Q (20 μM) selectively clear senCPCs, sparing non-senescent, cycling-competent CPCs, after 3 days of treatment[9]. We show here that this regime of D+Q treatment *in vitro* similarly leads to senCPC clearance and does not lead to the clearance of cycling-competent CPCs [Supplementary Figure 2]. iPSC-CM/senCPC co-cultures were treated after 7 days with the senolytics D+Q for 3 days, followed by a further 7 days of co-culture (total 17 days). D+Q treatment resulted in increased ($P < 0.01$) numbers of iPSC-CMs stained by crystal violet [Figure 2A] and increased ($P < 0.05$) iPSC-CMs positive for BrdU [Figure 2B], compared to co-culture for 17 days with senCPCs. We saw no changes in iPSC-CM survival or cell cycle activity when treated with D+Q alone (data
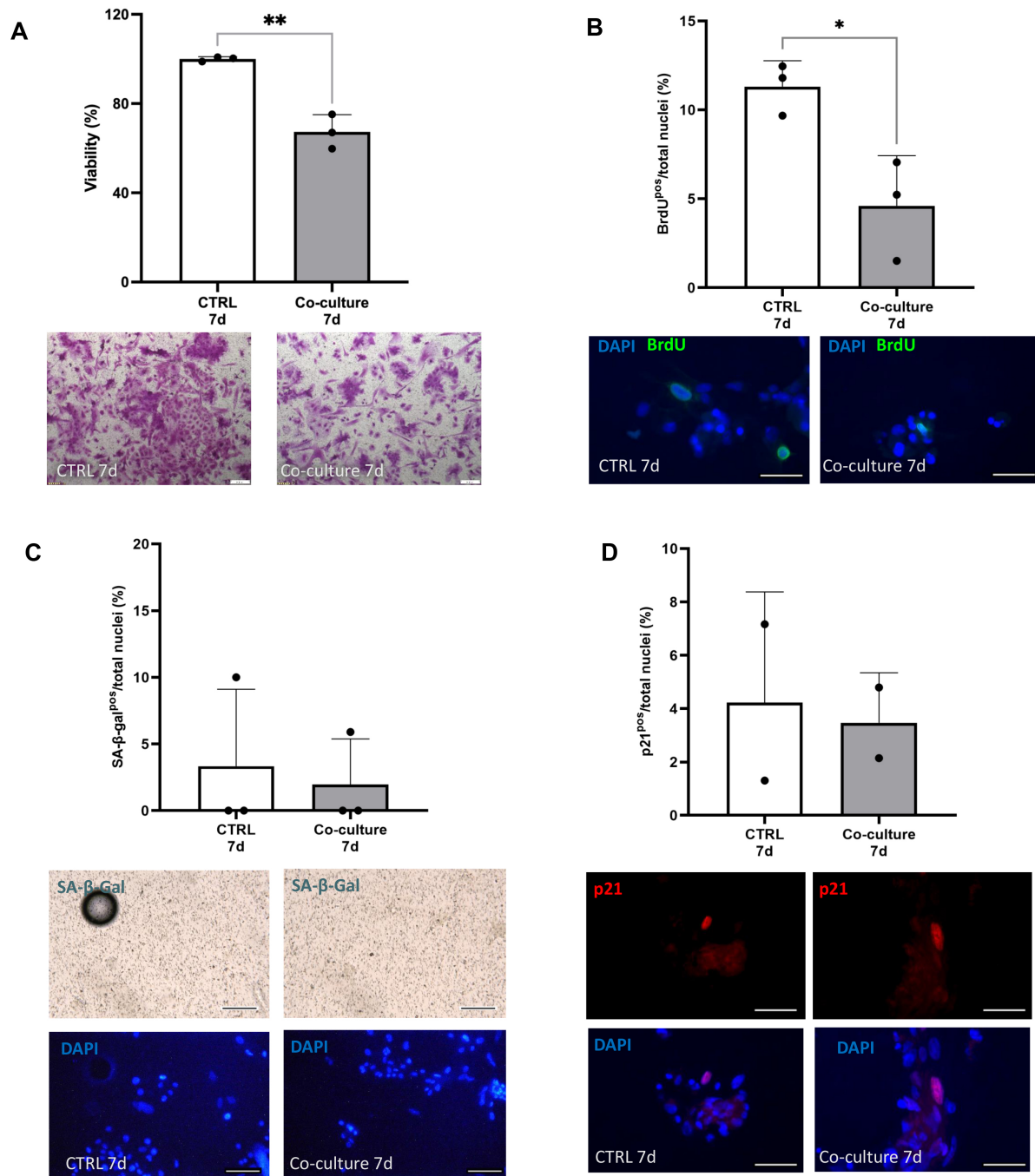
Figure 1. Co-culture with senCPCs decreases number of iPSC-CMs and their cell cycle activity. (A and B) iPSC-CM crystal violet staining (A) and BrdU-positive staining (B) when cultured alone (CTRL 7d) or co-cultured with senCPCs (Co-culture 7d). Data are Mean ± SD. Significance was determined by Student's t-test, *$P < 0.05$, ** $P < 0.01$. Individual data points represent independent replicates/wells. Representative field of view micrograph images of iPSC-CMs stained with crystal violet (A). Scale bar = 200 μm. Representative field of view micrograph images of iPSC-CMs labelled and immunostained with BrdU (green) and nuclei counterstained with DAPI (blue) (B). Scale bar = 50 μm. (C and D) SA-β-gal activity (C) and p21 expression (D) of iPSC-CMs when cultured alone (CTRL 7d) or co-cultured with senCPCs (Co-culture 7d). Data are Mean ± SD. Individual data points represent independent replicates/wells. Representative fields of view micrograph images of iPSC-CMs stained by enzymatic SA-β-gal assay (blue, upper panel) and nuclei counterstained with DAPI (blue, lower panel) (C). Scale bar = 100 μm. Representative fields of view micrograph images of iPSC-CMs immunostained for p21 (red) and nuclei counterstained with DAPI (blue) (D). Scale bar = 50 μm.
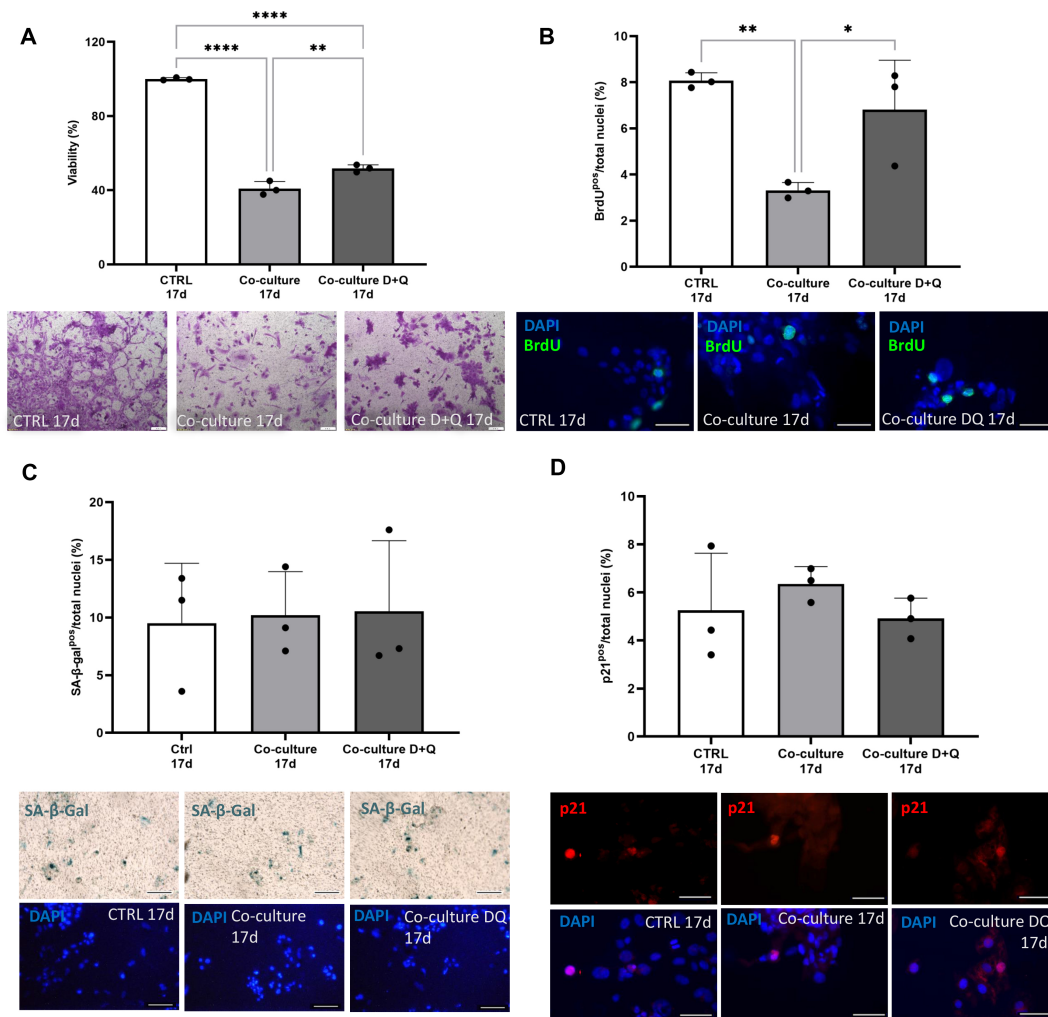
Figure 2. Senolytics D+Q rescue iPSC-CM number and cell cycle activity. (A and B) Percent of crystal violet stained iPSC-CMs (A) and BrdU-positive iPSC-CMs (B) when cultured alone (CTRL 17d), co-cultured with senCPCs (Co-culture 17d) or co-cultured with senCPCs and treated with D+Q (Co-culture D+Q 17d). Data are Mean ± SD. Significance was determined by ANOVA followed by Tukey's post-hoc test to identify the differences. *$P < 0.05$, **$P < 0.01$, ****$P < 0.0001$. Individual data points represent independent replicates/wells. Representative field of view micrograph images of iPSC-CMs stained with crystal violet (A). Scale bar = 200 μm. Representative field of view micrograph images of iPSC-CMs labelled and immunostained with BrdU (green) and nuclei counterstained with DAPI (blue) (B). Scale bar = 50 μm. (C and D) SA-β-gal activity (B) and p21 expression (D) of iPSC-CMs when cultured alone (CTRL 17d), co-cultured with senCPCs (Co-culture 17d) or co-cultured with senCPCs and treated with D+Q (Co-culture D+Q 17d). Data are Mean ± SD. Individual data points represent independent replicates/wells. Representative field of view micrograph images of iPSC-CMs stained by enzymatic SA-β-gal assay (blue, upper panel) and nuclei counterstained with DAPI (blue, lower panel) (C). Scale bar = 100 μm. Representative field of view micrograph images of iPSC-CMs immunostained for p21 (red) and nuclei counterstained with DAPI (blue) (D). Scale bar = 50 μm.

not shown). There were no changes in senescence markers, SA-β-gal or p21 expression, in iPSC-CMs co-cultured with senCPCs and then treated with senolytics D+Q, compared to iPSC-CMs co-cultured with senCPCs or iPSC-CMs cultured alone [Figure 2C and D]. To rule out that the co-culture condition and D+Q treatment may influence cell survival, we co-cultured adult rat ventricular cardiomyocytes, and used cardiomyocytes alone and those cultured with healthy, cycling-competent CPCs as the cell control. We showed that co-culture of adult rat ventricular rat cardiomyocytes with senCPCs led to decreased ($P = 0.007$) number of crystal violet stained cardiomyocytes, compared to cardiomyocytes co-cultured with healthy, cycling-competent CPCs. Then we showed that D+Q senolytic treatment of co-cultures of adult

ventricular rat cardiomyocytes with senCPCs or healthy, cycling-competent CPCs or cardiomyocytes alone showed no differences in crystal violet stained cardiomyocytes between groups. Therefore, the co-culture condition does not influence cell survival [Supplementary Figure 3].

Senolytics D+Q conditioned media rescue HUVEC number, migration and tube formation

We next measured the effects of senCPCs and D+Q treatment on HUVECs. When HUVECs were cultured in conditioned media from senCPCs, there was decreased ($P < 0.05$) number of crystal violet stained HUVECs [Figure 3A] and Ki67-positive HUVECs [Figure 3B], compared to HUVECs cultured in normal growth media. When HUVECs were treated with D+Q conditioned media, the number of crystal violet stained HUVECs returned to control normal growth media levels ($P < 0.05$) [Figure 3A]. The number of Ki67-positive HUVECs increased [Figure 3B], yet this was not significant compared to HUVECs cultured in senCPC conditioned media, and still significantly decreased ($P < 0.0001$) compared to normal growth media. As a measure of HUVEC migration, we performed the scratch wound assay. Treatment of HUVECs with senCPC conditioned media led to decreased ($P < 0.0001$) number of HUVECs that crossed into the scratched area. When D+Q conditioned media was supplemented, the number of HUVECs that crossed into the scratched area increased ($P < 0.01$), compared to when treated with senCPC conditioned media, but was still significantly decreased ($P < 0.0001$) compared to control normal growth media [Figure 3C]. Finally, we measured the effects of senCPCs and D+Q treatment on HUVECs in the Matrigel tube network formation assay. Treatment of HUVECs with senCPC conditioned media led to decreased ($P < 0.05$) tube formation compared to normal growth media control [Figure 3D]. Tube formation increased ($P < 0.05$) when HUVECs were supplemented with D+Q conditioned media, and there was no significant difference between normal growth medium and D+Q conditioned media [Figure 3D].

D+Q treatment rescues HUVEC number and tube formation in co-cultures of SenHUVECs with HUVECs

Next, we tested the effects of co-culture of senHUVECs and D+Q treatment on HUVECs. 24 h of dox induced HUVECs into a senescent state 21 days later [Supplementary Figure 4]. When senescent HUVECs (senHUVECs) were co-cultured with non-senescent, cycling-competent HUVECs for 7 days, there was decreased ($P < 0.05$) number of the cycling competent HUVECs that stained for crystal violet [Figure 4A] and those that were BrdU-positive [Figure 4B], compared to cycling competent HUVECs cultured alone in control growth media. Treatment with senolytics D+Q cleared the senHUVECs [Supplementary Figure 5] in the co-culture and ameliorated the number of crystal violet stained cycling competent HUVECs ($P < 0.05$), but not BrdU positive HUVECs, [Figure 4C and D]. Next, we performed the Matrigel tube network formation assay. Treatment of HUVECs with conditioned media from senHUVECs led to decreased ($P < 0.0001$) tube formation [Figure 4E]. Treatment of HUVECs with D+Q conditioned media improved ($P < 0.01$) HUVEC tube formation, compared to senHUVEC conditioned media; however, the tube formation was still significantly decreased ($P < 0.05$) compared to normal control growth medium [Figure 4E]. Finally, we showed that treatment of HUVECs with conditioned media from senHUVECs decreased ($P < 0.0001$) HUVEC migration compared to normal control growth medium [Figure 4F]. However, treatment with D+Q did not significantly rescue the effect on migration [Figure 4F].

Senolytic D+Q treatment abrogates the SASP

Luminex analysis of the conditioned media at 7 and 17 days of exposure to senCPCs co-cultured with iPSC-CMs revealed upregulation ($P < 0.05$) of 6 out of 8 SASP factors: IL-6, IL-8, CCL11, CXCL5, CXCL1 and CCL7 [Figure 5A]. Following the application of senolytics D+Q, the levels of these SASP factors, except
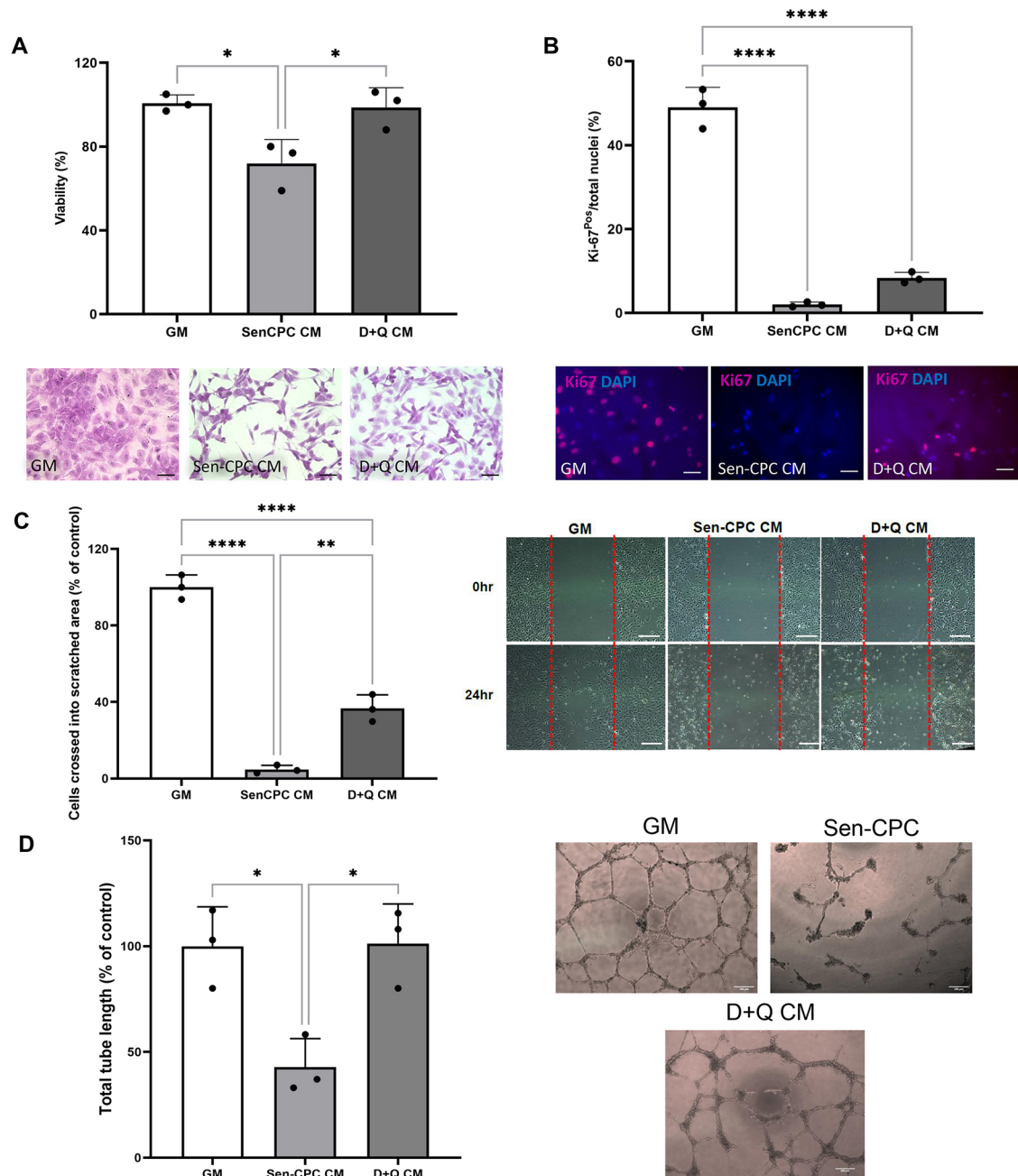
Figure 3. Senolytics D+Q conditioned media rescue HUVEC number, migration and tube formation. (A and B) Percent of crystal violet stained HUVECs (A) and Ki67-positive HUVECs (B) when cultured in normal growth media (GM), senCPC conditioned media (SenCPC CM), and D+Q conditioned media (D+Q CM). Data are Mean ± SD. Significance was determined by ANOVA followed by Tukey's post-hoc test to identify the differences. ****$P < 0.0001$, *$P < 0.05$. Individual data points represent independent replicates/wells. Representative field of view micrograph images of HUVECs stained with crystal violet (A) and Ki67 (red; B). Nuclei counterstained with DAPI (blue). Scale bar = 50 μm. (C) HUVEC migration measured by the scratch assay when supplemented with normal growth media (GM), senCPC conditioned media (SenCPC CM), and D+Q conditioned media (D+Q CM) for 24 h. Data are Mean ± SD% of control (GM). Significance was determined by ANOVA followed by Tukey's post-hoc test to identify the differences ****$P < 0.0001$, **$P < 0.01$. Representative field of view micrograph images of the scratch (red dotted lines) in the different media conditions. (D) Total tube length formed by HUVECs when cultured in normal growth media (GM), senCPC conditioned media (Sen-CPC CM), and D+Q conditioned media (D+Q CM). Data are Mean ± SD% of control (GM). Significance was determined by ANOVA followed by Tukey's post-hoc test to identify the differences. *$P < 0.05$. Individual data points represent independent replicates/wells. Representative field of view micrograph images of HUVEC tube formation. Scale bar = 200 μm.
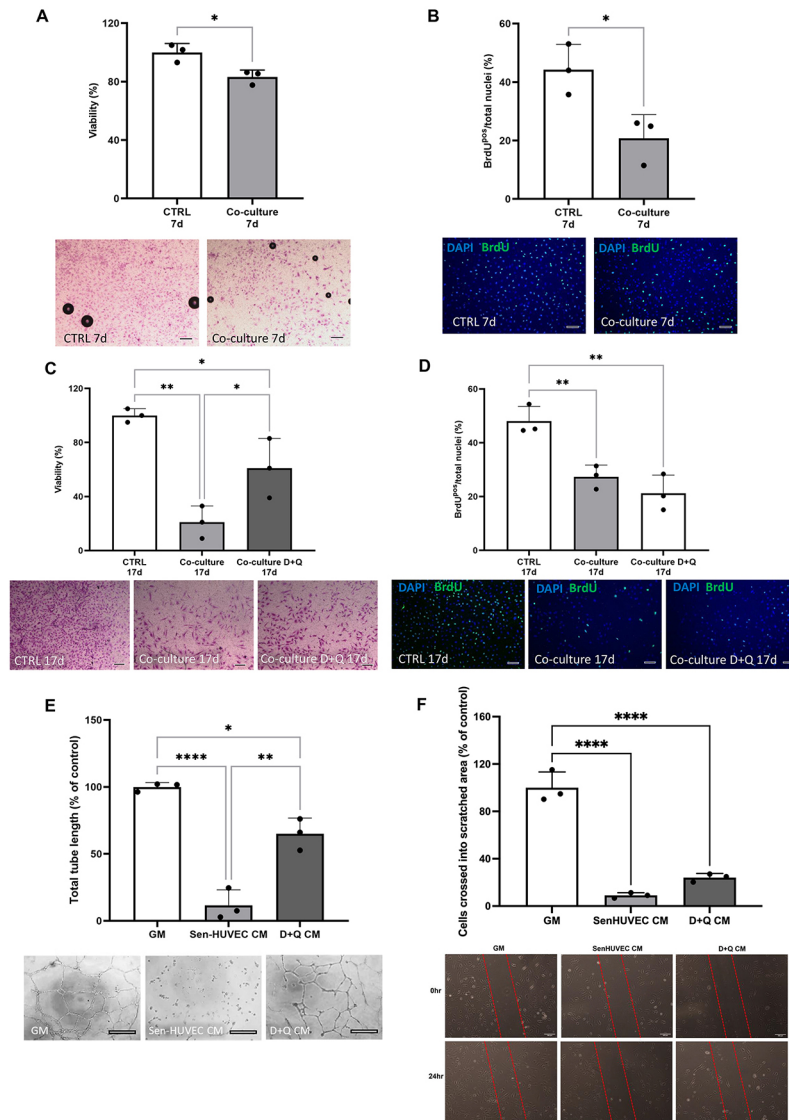
Figure 4. Senolytics D+Q treatment of SenHUVECs with HUVECs co-culture rescues HUVEC number and tube formation. (A and B) Percent of crystal violet stained HUVECs (A) and BrdU-positive HUVECs (B) when cultured alone (CTRL 7d) or co-cultured with senHUVECs (Co-culture 7d). Data are Mean ± SD. Significance was determined by Student's t-test, *P < 0.05. Individual data points represent independent replicates/wells. Representative field of view micrograph images of HUVECs stained with crystal violet (A). Scale bar = 200 μm.Representative field of view micrograph images of HUVECs labelled and immunostained with BrdU (green) and nuclei counterstained with DAPI (blue) (B). Scale bar = 100 μm. (C and D) Percent of crystal violet stained HUVECs(C) and BrdU-positive HUVECs (D) when cultured alone (CTRL 17d), co-cultured with senHUVECs (Co-culture 17d) or co-cultured with senHUVECs and treated with D+Q (Co-culture D+Q 17d). Data are Mean ± SD. Significance was determined by ANOVA followed by Tukey's post-hoc test to identify the differences. **P < 0.01, *P < 0.05. Individual data points represent independent replicates/wells. Representative field of view micrographimages of HUVECs stained with crystal violet (C) and BrdU (green; D). Nuclei counterstained with DAPI (blue). Scale bar = 200 μm in (C) and 100 μm in (D). (E) Total tube length formed by HUVECs when cultured in normal growth medium (GM), senHUVEC conditioned medium (SenHUVEC CM) or senHUVEC treated with D+Q conditioned medium (D+Q CM). Data are Mean ± SD% of control (GM). Significance was determined byANOVA followed by Tukey's post-hoc test to identify the differences. ****P < 0.0001, **P < 0.01, *P < 0.05.Individual data points represent independent replicates/wells. Representative field of view micrograph images of HUVEC tube formation. Scale bar = 500 μm. (F) HUVEC migration measured by the scratch assay when supplemented with normal growth media (GM), senHUVEC conditioned media (SenHUVEC CM), or D+Q conditioned medium (D+Q CM) for 24 h. Data are Mean ± SD% of control (GM). Significance was determined by ANOVA followed by Tukey's post-hoc test to identify the differences ****P < 0.0001. Representative field of view micrograph images of the scratch (red dotted lines) in the different media conditions.

SenCPC + iPSC-CM co-culture
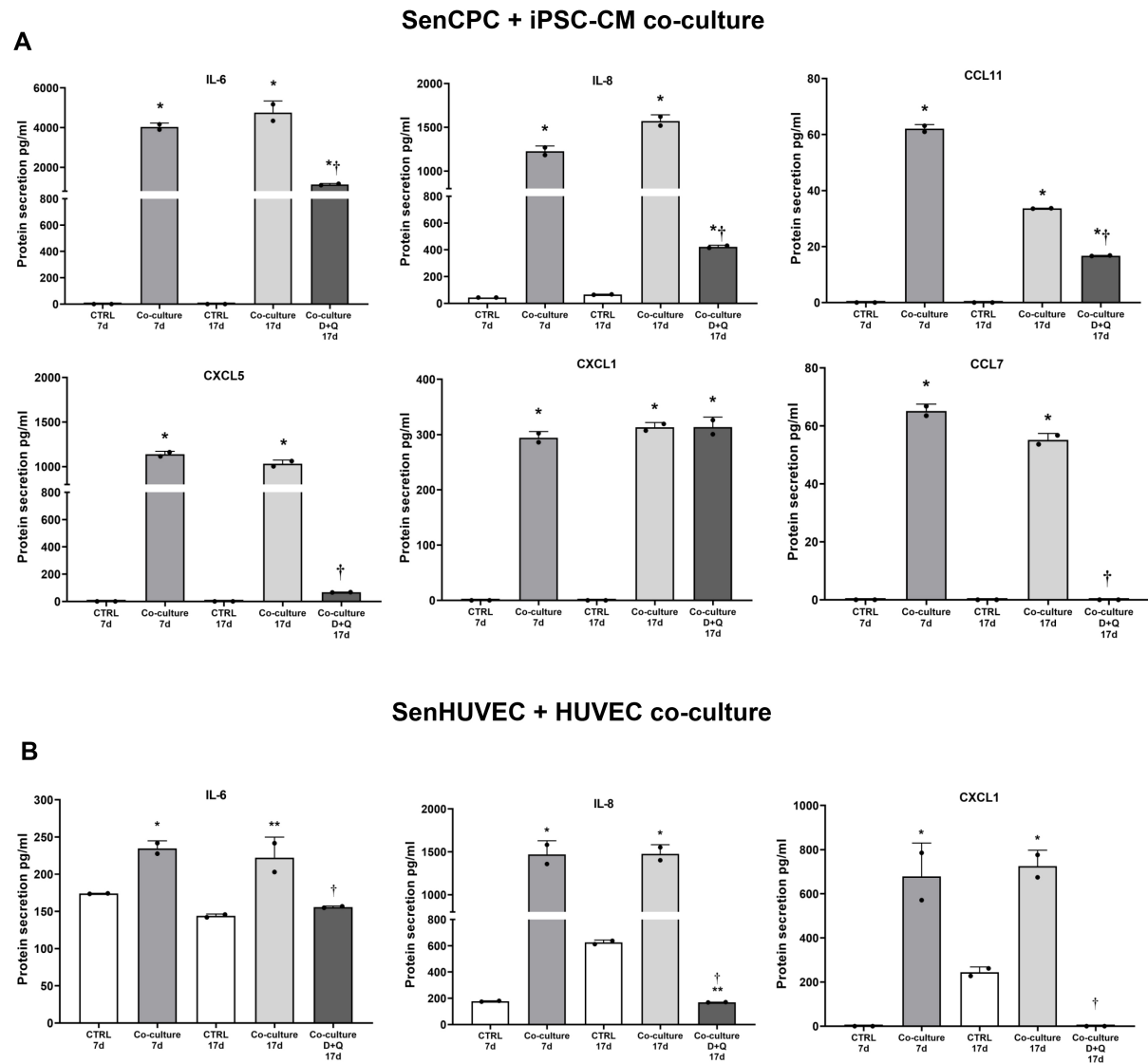

SenHUVEC + HUVEC co-culture

Figure 5. Senolytic D+Q treatment abrogates the SASP. (A) Secretion of SASP proteins, IL-6, IL-8, CCL11, CXCL5, CXCL1, CCL7, in media of iPSC-CMs cultured alone for 7 days (CTRL 7d), co-cultured with senCPCs for 7 days (Co-culture 7d), cultured alone for 17 days (CTRL 17d), co-cultured with senCPCs for 17 days (Co-culture 17d), or co-cultured with senCPCs and treated with D+Q (Co-culture D+Q 17d). Data are Mean ± SD. Significance was determined by ANOVA followed by Tukey's post-hoc test to identify the differences. *$P < 0.05$ *vs.* 7d and 17d CTRL; †$P < 0.05$ *vs.* 7d and 17d co-culture. Individual data points represent independent replicates/wells. (B) Secretion of SASP proteins, IL-6, IL-8 and CXCL1, in medium of HUVECs cultured alone for 7 days (CTRL 7d), co-cultured with senHUVECs for 7 days (Co-culture 7d), cultured alone for 17 days (CTRL 17d), co-cultured with senHUVECs for 17 days (Co-culture 17d), or co-cultured with senHUVECs and treated with D+Q (Co-culture D+Q 17d). Data are Mean ± SD. Significance was determined by ANOVA followed by Tukey's post-hoc test to identify the differences. *$P < 0.05$ *vs.* 7d and 17d CTRL; **$P < 0.05$ *vs.* 17d CTRL; †$P < 0.05$ *vs.* 7d and 17d co-culture. Individual data points represent independent replicates/wells.

CXCL1, were decreased ($P < 0.05$) [Figure 5A]. Across all conditions, the levels of IL-1β and TNFα were low or negligible, respectively. Luminex analysis of the conditioned media at 7 and 17 days exposure to senescent HUVECs co-cultured with HUVECs revealed upregulation ($P < 0.05$) of 3 out of 8 SASP factors: IL-6, IL-8, and CXCL1 [Figure 5B]. Following the application of senolytics D+Q, the levels of these SASP factors were decreased ($P < 0.05$) [Figure 5B]. Across all conditions, the levels of IL-1β, TNFα, CCL11, CXCL5, and CCL7 were negligible.

DISCUSSION

The present findings show that co-culture of human senescent cells with human iPSC-derived cardiomyocytes and endothelial cells leads to decreased survival and cell cycle activity. Moreover, endothelial cells show impaired tube formation and migration. Senolytics D+Q improve human iPSC-derived cardiomyocyte survival and DNA synthesis by eliminating senescent cells. Senolytics D+Q also improve human endothelial cell survival, migration, and tube formation. The mechanism of action supports the secretion of a SASP by senescent cells (especially IL-6, IL-8), which was abrogated with D+Q treatment.

In cardiovascular disease (CVD), senescence and the abundance of senescent cells promotes a pathological inflammatory microenvironment, exacerbating disease progression and escalating disease severity. The SASP has been shown to induce bystander effects, particularly on the viability and proliferation of neighbouring cells, and inducing senescence[13]. The present findings corroborate previous findings that senescent cells have a SASP, and clearance of senescent cells using a combination of senolytics D+Q abrogates the SASP, and as shown here, its detrimental effect on iPSC-CMs and HUVECs.

A plethora of studies are emerging showing senescent cells and their SASP lead to decreased HUVEC, CPC or MSC survival and proliferation[9,14-16], and inhibit HUVEC angiogenic potential[17]. Moreover, the SASP of old cardiomyocytes reduced the proliferation of neonatal fibroblasts and increased the expression of α-smooth muscle actin (αSMA), an indicator of myofibroblast activation[11]. *In vivo* work corroborates the detrimental effect of the SASP on cardiac repair and regeneration. Dookun *et al.* found that senescent cells and their SASP was associated with reduced myocardial vascularisation and increased scar size after ischaemia reperfusion[18]. Work from our group showed that transplantation of senescent CPCs into the myocardial infarcted mouse heart increased LV fibrosis and stalled cardiac repair and regeneration, unlike when healthy, proliferative human CPCs were injected[9]. Also, senescence and SASP are the main mechanisms of cardiac reparative defects in Diabetes[19]. Altogether, the SASP from different cell types can reduce the survival and proliferation of multiple cells present in the heart that play a role in cardiac repair, remodelling, and regeneration.

The present findings support that the effects of the SASP are cell-type specific, with senCPCs secreting a greater amount of SASP factors than senHUVECs. This led to a more robust effect of D+Q treatment in the senCPCs co-culture on HUVEC survival, migration and tube formation [Figure 3] compared to the senHUVECs co-culture condition [Figure 4]. However, D+Q treatment was not able to ameliorate HUVEC cell cycle activity in either senCPC or senHUVEC co-culture conditions.

Previous work has demonstrated that senescent cells resident in different tissues are substantially distinct in their transcriptomic and SASP profiles, consistent with a tissue-of-origin programme[20]. Comparisons of senescent preadipocytes, endothelial cells, myoblasts, fibroblasts, and epithelial cells reveal differences in the extent of upregulation of SASP factors[21], with senescent endothelial cells and preadipocytes having a greater SASP factor expression than epithelial cells or myoblasts[20]. Moreover, the cardiomyocytes of aged mouse hearts activate a non-typical SASP, with increased expression and secretion of Edn3, Tgfβ2 and Gdf15, which have both autocrine and paracrine effects[11]. Higher SASP expression, like that shown here for CPCs, implies that some senescent cells may contribute more to chronic inflammation and organismal age-related dysfunction than others[20].

Senescent cells and their SASP present a promising therapeutic target to rejuvenate the heart's reparative potential, and senolytics are one such promising therapeutic. Previous work has shown that application of senolytics D+Q can abrogate the SASP and improve CPC survival and proliferation[9]. Then, eliminating

senescent cells in aged mice using D+Q rejuvenated the heart's regenerative potential with CPC activation, new cardiomyocyte formation, and improved cardiac function[9,10]. Likewise, the elimination of senescent cells, either genetically or through administration of the senolytic navitoclax, led to decreased cardiomyocyte hypertrophy, fibrosis and increased cardiomyocyte formation in the aged mouse heart[11]. Senolytics have shown therapeutic potential following cardiac injury. Dookun *et al.* found that navitoclax treatment attenuated post-ischemia-reperfusion inflammatory/SASP response leading to improved cardiac function, reduced scar size, and increased angiogenesis[18]. Moreover, navitoclax clearance of senescent cells improved myocardial remodelling and diastolic function, as well as overall survival following MI in aged mice[22]. Furthermore, we show that senescent cells promote ischemic ageing in the female heart and senescent cell clearance by D+Q improves cardiac remodeling and function after myocardial infarction in aged female mice[23].

Results from the present study fall short of showing that the SASP can switch otherwise healthy cells to a senescent phenotype. In the present study, there were no changes to iPSC-CM senescent marker expression, p21 and SA-β-gal, after 7 and 17 days of co-culture with senescent cells or after D+Q. These findings contradict previous work that showed CPCs co-cultured with senescent CPCs increased the expression of p16[INK4A], SA-β-gal and γH2AX, and D+Q treatment attenuated the number of p16[INK4A] and SA-β-gal CPCs[9]. The spread of senescence to recipients' cells has also been observed after transplanting senescent adipocyte progenitors *in vivo*[6], but not in the heart. Therefore, the SASP stimulus *in vitro* may not be great enough in magnitude or duration to induce a senescent phenotype to unique cardiac immature cell types, such as iPSC-CMs.

The present findings showed that senCPCs co-culture led to decreased iPSC-CM DNA synthesis and D+Q treatment improved iPSC-CM DNA synthesis. As the majority of adult cardiomyocytes are post-mitotic and unable to re-enter the cell cycle, the present findings do not support the action of senolytics on the proliferation of adult cardiomyocytes. Instead, iPSC-CMs are an immature fetal phenotype and reflect more the cardiomyocyte population that retains some proliferative potential in the adult heart[12]. Therefore, senolytics D+Q could offer therapeutic potential in improving endogenous cardiac regeneration mechanisms and also cell therapy transplantation *in vivo*.

An accumulation of senescent cells is associated with the declining function of the aged cardiovascular system and many age-related CVDs, including atherosclerosis, arterial calcification, hypertension, aortic aneurysm, vessel stenosis, and heart failure. Therefore, senescent cells present a promising drug target to alleviate CVD. As senolytics selectively eliminate senescent cells while leaving non-senescent cells unaffected, they allow the targeting of a central pathway to many CVDs, treating the pathologies together rather than individually. Furthermore, the treatment need only be administered intermittently (e.g., monthly) as senolytics are administered in a hit-and-run approach[24], which would further minimise the possibility of adverse side effects while increasing the compliance of the patients[25]. Senolytics could simultaneously target co-morbidities such as atherosclerosis[26], diabetes[27,28], and adverse cardiac remodelling[10]. Most importantly, they present the opportunity to prevent the disease before its manifestation by breaking down the mechanistic relationship between ageing and increased CVD risk. Therefore, senescence presents a common therapeutic target whereby these age-related cardiovascular deteriorations may be simultaneously alleviated. By clearing senescent cells, disease onset could be delayed, progression hindered, and disease severity significantly improved.

Limitations: The present findings fall short of validating improved angiogenesis (migration, tube formation) with D+Q treatment through additional methods such as protein or gene expression. The number of

independent replicates was only 3 for the *in vitro* assays and 2 for the Luminex SASP multiplexing array. Further n should be applied to validate the Luminex data. Even though we showed that the co-culture condition does not influence cell survival, this was carried out on the co-culture of senCPCs or non-senescent CPCs with adult rat ventricular cardiomycytes. Similar experiments using non-senescent CPCs and HUVECs co-cultured with iPSC-CMs or HUVECs for all tested parameters should be carried out. Finally, the selectivity of different senolytics (navitoclax, fisetin) on clearing senCPCs and senHUVECs and their effects on cardiomyocytes and endothelial cells should be determined.

In conclusion, the present findings show the therapeutic potential of senolytics D+Q in rejuvenating the reparative activity of human iPSC-derived cardiomyocytes and endothelial cells. These results open the path to further studies on using senolytic therapy in age-related cardiovascular deterioration and rejuvenation.

DECLARATIONS

Authors' contributions
Collection and/or assembly of data, data analysis and interpretation, manuscript writing: Sunderland P, Alshammari L, Ambrose E
Data collection, analysis and interpretation, manuscript writing: Torella D
Conception and design, data analysis and interpretation, manuscript writing, final approval of manuscript: Ellison-Hughes GM
All authors read and approved the final manuscript.

Availability of data and materials
The datasets generated and analysed during the current study are available from the corresponding author upon reasonable request.

Conflicts of interest
All authors declared that there are no conflicts of interest.

Ethical approval and consent to participate
As previously reported[9], cardiac progenitor cells (CPCs) were isolated from a right atrial appendage myocardial sample (~200 mg) obtained from a subject with cardiovascular disease undergoing valve replacement surgery. Informed consent was given to take part in the study and the study was approved by both the Institutional and National Research Ethics Committees (NREC #08/H1306/91). Human iPSC-Derived Ventricular Cardiomyocytes (iPSC-CMs) were purchased from Axol. HUVECs were purchased from Lonza.

Consent for publication
Not applicable.

REFERENCES

1. United Nations department of economic and social affairs, population division. world population ageing 2020 highlights. Available from: https://www.un.org/development/desa/pd/sites/www.un.org.development.desa.pd/files/undesa_pd-2020_world_population_ageing_highlights.pdf [Last accessed on 17 Apr 2023].

2. World Health Organization. World report on ageing and health. 2015. Available from: https://apps.who.int/iris/handle/10665/186463 [Last accessed on 17 Apr 2023].

3. Tchkonia T, Kirkland JL. Aging, cell senescence, and chronic disease: emerging therapeutic strategies. *JAMA* 2018;320:1319-20. DOI PubMed

4. Coppé JP, Patil CK, Rodier F, et al. Senescence-associated secretory phenotypes reveal cell-nonautonomous functions of oncogenic RAS and the p53 tumor suppressor. *PLoS Biol* 2008;6:2853-68. DOI PubMed PMC

5. Wang B, Liu Z, Chen VP, et al. Transplanting cells from old but not young donors causes physical dysfunction in older recipients. *Aging Cell* 2020;19:e13106. DOI PubMed PMC

6. Xu M, Pirtskhalava T, Farr JN, et al. Senolytics improve physical function and increase lifespan in old age. *Nat Med* 2018;24:1246-56. DOI PubMed PMC

7. Ellison-Hughes GM. Senescent cells: targeting and therapeutic potential of senolytics in age-related diseases with a particular focus on the heart. *Expert Opin Ther Targets* 2020;24:819-23. DOI PubMed

8. Kirkland JL, Tchkonia T. Cellular senescence: a translational perspective. *EBioMedicine* 2017;21:21-8. DOI PubMed PMC

9. Lewis-McDougall FC, Ruchaya PJ, Domenjo-Vila E, et al. Aged-senescent cells contribute to impaired heart regeneration. *Aging Cell* 2019;18:e12931. DOI PubMed PMC

10. Zhu Y, Tchkonia T, Pirtskhalava T, et al. The Achilles' heel of senescent cells: from transcriptome to senolytic drugs. *Aging Cell* 2015;14:644-58. DOI PubMed PMC

11. Anderson R, Lagnado A, Maggiorani D, et al. Length-independent telomere damage drives post-mitotic cardiomyocyte senescence. *EMBO J* 2019;38:e100492. DOI PubMed PMC

12. Salerno N, Salerno L, Marino F, et al. Myocardial regeneration protocols towards the routine clinical scenario: an unseemly path from bench to bedside. *EClinicalMedicine* 2022;50:101530. DOI PubMed PMC

13. Acosta JC, Banito A, Wuestefeld T, et al. A complex secretory program orchestrated by the inflammasome controls paracrine senescence. *Nat Cell Biol* 2013;15:978-90. DOI PubMed PMC

14. Suvakov S, Cubro H, White WM, et al. Targeting senescence improves angiogenic potential of adipose-derived mesenchymal stem cells in patients with preeclampsia. *Biol Sex Differ* 2019;10:49. DOI PubMed PMC

15. Zhang B, Zhang J, Zhu D, Kong Y. Mesenchymal stem cells rejuvenate cardiac muscle after ischemic injury. *Aging* 2019;11:63-72. DOI PubMed PMC

16. Parvizi M, Ryan ZC, Ebtehaj S, Arendt BK, Lanza IR. The secretome of senescent preadipocytes influences the phenotype and function of cells of the vascular wall. *Biochim Biophys Acta Mol Basis Dis* 2021;1867:165983. DOI PubMed

17. Wong PF, Tong KL, Jamal J, Khor ES, Lai SL, Mustafa MR. Senescent HUVECs-secreted exosomes trigger endothelial barrier dysfunction in young endothelial cells. *EXCLI J* 2019;18:764-76. DOI PubMed PMC

18. Dookun E, Walaszczyk A, Redgrave R, et al. Clearance of senescent cells during cardiac ischemia-reperfusion injury improves recovery. *Aging Cell* 2020;19:e13249. DOI PubMed PMC

19. Marino F, Scalise M, Salerno N, et al. Diabetes-induced cellular senescence and senescence-associated secretory phenotype impair cardiac regeneration and function independently of age. *Diabetes* 2022;71:1081-98. DOI PubMed PMC

20. Tripathi U, Misra A, Tchkonia T, Kirkland JL. Impact of senescent cell subtypes on tissue dysfunction and repair: importance and research questions. *Mech Ageing Dev* 2021;198:111548. DOI PubMed PMC

21. Schafer MJ, Zhang X, Kumar A, et al. The senescence-associated secretome as an indicator of age and medical risk. *JCI Insight* 2020;5:133668. DOI PubMed PMC

22. Walaszczyk A, Dookun E, Redgrave R, et al. Pharmacological clearance of senescent cells improves survival and recovery in aged mice following acute myocardial infarction. *Aging Cell* 2019;18:e12945. DOI PubMed PMC

23. Salerno N, Marino F, Scalise M, et al. Pharmacological clearance of senescent cells improves cardiac remodeling and function after myocardial infarction in female aged mice. *Mech Ageing Dev* 2022;208:111740. DOI

24. Hickson LJ, Langhi Prata LGP, Bobart SA, et al. Senolytics decrease senescent cells in humans: Preliminary report from a clinical trial of Dasatinib plus Quercetin in individuals with diabetic kidney disease. *EBioMedicine* 2019;47:446-56. DOI PubMed PMC

25. Masnoon N, Shakib S, Kalisch-Ellett L, Caughey GE. What is polypharmacy? *BMC Geriatr* 2017;17:230. DOI PubMed PMC

26. Roos CM, Zhang B, Palmer AK, et al. Chronic senolytic treatment alleviates established vasomotor dysfunction in aged or atherosclerotic mice. *Aging Cell* 2016;15:973-7. DOI PubMed PMC

27. Marino F, Salerno N, Scalise M, et al. Streptozotocin-induced type 1 and 2 diabetes mellitus mouse models show different functional, cellular and molecular patterns of diabetic cardiomyopathy. *Int J Mol Sci* 2023;24:1132. DOI PubMed PMC

28. Molinaro C, Salerno L, Marino F, et al. Unraveling and targeting myocardial regeneration deficit in diabetes. *Antioxidants* 2022;11:208. DOI PubMed PMC